PHYSICAL REVIEW A VOLUME 16, NUMBER 3 SEPTEMBER 1977

Straggling of fast electrons in aluminum foils observed in high-voltage electron microscopy (0.3–1.2 MV)

J. Ph. Perez, J. Sevely, and B. Jouffrey
Laboratoire d'Optique Electronique du CNRS, 29, rue Jeanne Marvig-31055 Toulouse Cedex, France
(Received 10 December 1976; revised manuscript received 30 March 1977)

By using an electron-energy analyzer adapted on a high-voltage electron microscope, energy-loss straggling of relativistic electrons (0.3–1.2 MeV) through 1- to 8.5-μm-thick aluminum foils has been investigated in the energy range 0–4000 eV. The energy resolution of the analysis is 3 eV. The experimental values of the most probable energy loss ΔE_p and of the full width at half maximum $\Delta E_{1/2}$ are interpreted by taking account of the effects of all-order terms in the Landau theory. This latter is revisited by introducing the relativistic Bethe cross section associated with all kinds of excitation processes including plasmons; it is observed that plasmon influence is negligible in this thickness and energy range.

I. INTRODUCTION

The energy-loss straggling suffered by particles through matter has been considered by many authors, mainly in connection with heavy particles like protons and positive pions.[1-7] The loss distribution for very fast heavy particles was generally concluded to be in good agreement with the Landau theory[8] and with its generalization proposed by Vavilov[9] when the mean energy loss in the target was not very small compared to the maximum energy transfer in a single collision, but small compared to the incident energy. The most probable energy loss ΔE_p and the full width at half maximum (FWHM) $\Delta E_{1/2}$ of the straggling remained within a few percent experimental uncertainty. For protons less than 20 MeV, a difference was observed between theory and experiments, the discrepancy increasing with decreasing incident proton energy.[3]

For electrons, the measurements are less numerous. Aitken *et al.*[1] observed for very fast electrons [458-MeV electrons through Si(Li) detectors] a spectrum larger than the theoretical one given by Landau. More recently, Nagata *et al.*[10] studied 100-MeV electrons through gas samples and found disagreement between the FWHM of the ionization loss distribution and the Landau theory and even with the correction of Blunck and Leisegang,[11] who took account of the second-order moment in mechanical resonance energy transfer.

In electron microscopy, energy losses suffered by electrons give a blurring of the images. In order to understand the variation of this effect with the energy of incident electrons in the case of high-voltage electron microscopy we studied the energy loss of electrons in the kinetic-energy range 0.3–1.2 MeV using specimens a few micrometers thick. In most of the previously published experiments, the accuracy was limited by the energy spread of the incident beam which generally was about 1%.[6,7] In the field of electron microscopy, some results have already been reported by Considine *et al.*[12] Using a magnetic analyzer[13] adapted on the 1.2-MV electron microscope of our laboratory,[14] we have extended those measurements into a higher-energy range and with a better energy resolution, about 3×10^{-6}.

For one-MeV electrons and aluminum foils a few micrometers thick, the difference between the Landau and Vavilov treatments is insignificant.[15] Recently Bichsel[16,17] has proposed a better approximation of the energy-loss distribution for heavy particles by introducing moments of higher orders calculated in the first Born approximation using a hydrogenic wave function. In our approach we have investigated the contribution of all moments by using the mean free paths corresponding to the atomic excitations and including plasmons which were measured with a reasonable accuracy in samples a few thousand angstroms thick.[18,19]

In this paper we discuss the results of measurements performed on the energy-loss spectra obtained with aluminum foils, and compare them with the theory. Since the experimental values of ΔE_p and $\Delta E_{1/2}$ are about a few hundred eV, the distortion of the energy-loss distribution, because of the small energy spread of the incident electron beam (3 eV) and of the resolution of the analyzer, is negligible, so it is not necessary to make any correction to the observed values as in several previous experiments.[1,6] The electron microscope also allows control of the effect of the maximum electron scattering angle α which is defined by the objective aperture. A particular advantage of the technique is that the area of the object corresponding to the spectrum can be known exactly.

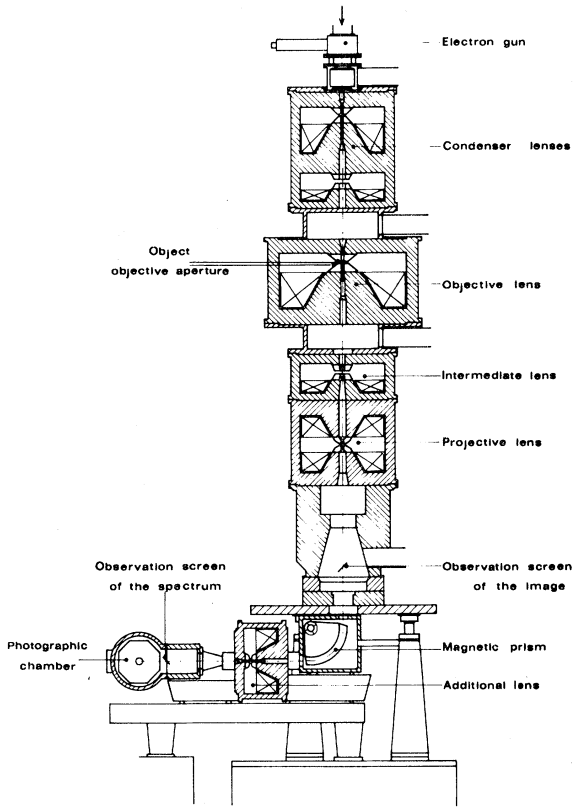

FIG. 1. Cross section of the high-voltage electron analyzer.

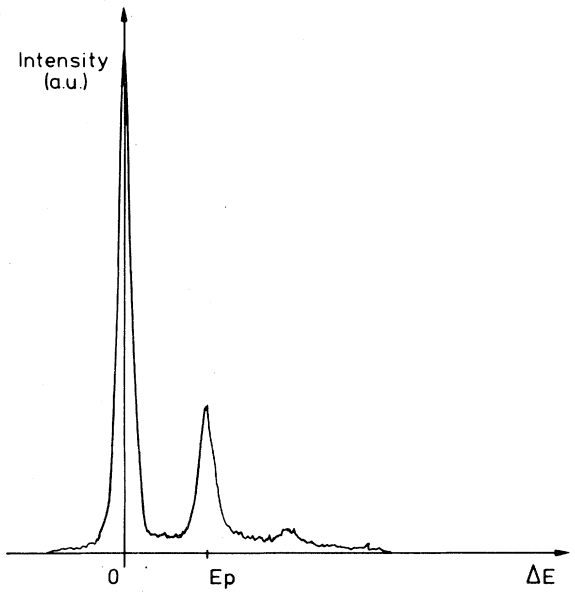

FIG. 2. Electron-energy-loss spectrum in a thin aluminum foil: $E_p \simeq 15$ eV and the FWHM of the no loss peak is $\simeq 3$ eV.

II. EXPERIMENTAL ARRANGEMENT AND PROCEDURE

The experimental arrangement for the energy analysis of the electrons transmitted by the object is a $\frac{1}{2}\pi$ magnetic prism adapted after the screen of the electron microscope (Fig. 1). The energy analysis is performed on a selected area of the image on the screen of the microscope: it corresponds to a 2×10^{-2}-μm^2 area of the sample. In order to avoid the limitation of the resolving power of the analyzer due to the spatial resolution of the detector, the spectrum at the output of the prism is magnified by an additional magnetic lens. In these experiments, the spectra were recorded on a photographic plate and the values of interest were measured by microdensitomer traces. Only those corresponding to an optical density range 0–1 were kept. The energy resolution of the analyzer was checked on aluminum plasmon spectra as shown in Fig. 2. It is given by the full width at half maximum of the no-loss peak (3 eV) as deduced from the position of the first plasmon peak for which $E_p=\hbar\omega_p\simeq15$ eV. The energy calibration of the system was performed by changing the accelerating voltage V of the primary electron beam. It shows that the dispersion varies linearly in the 0–2000-eV energy range.

Energy losses of electrons through 1- to 8.5-μm-thick aluminum foils were measured as the kinetic energy of incident electrons was varied from 0.3 MeV up to 1.2 MeV. These thicknesses were determined to ±5% precision by the usual weighing method and also by means of a pneumatic comparator. Up to 1 μm the number and the relative intensity of plasmon peaks in the spectra allowed us to control those measurements that, on the other hand, could be extrapolated to higher thicknesses.

The α aperture value chosen for the measurements reported here, $\alpha=40$ mrad, was sufficiently large so that the energy-loss distributions were monotonic. The characteristic variations were smeared into the background mainly because of the continuous single electron collisions. They are readily revealed by reducing α as shown in Fig. 3(a) where the visibility of plasmon lines confirms that plasmon is a small angle scattering excitation. This observation suggests that plasmons contribute to the straggling and that their contribution should be investigated.

III. THEORY

The probability $f(x,\Delta E)$ that an electron with an incident energy E, going through an x-μm-thick layer, will lose an amount of energy ΔE, obeys the Boltzmann equation[8]

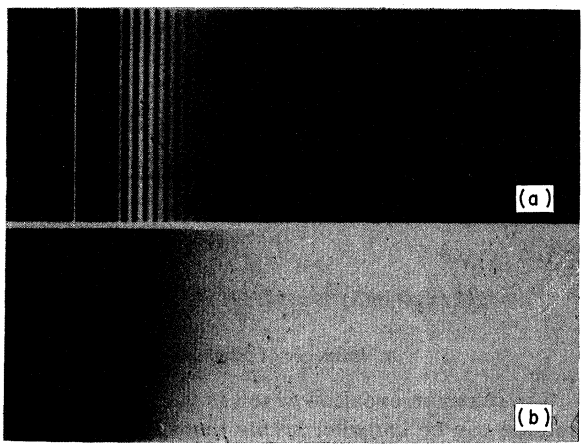

FIG. 3. Influence of the maximal scattering angle on the energy-loss spectra obtained with samples a few microns thick: Electron kinetic energy, 1 MeV; thickness, 3 μm. (a) $\alpha = 0.5$ mrad. In this micrograph the no loss line has been superimposed in the spectrum; (b) $\alpha = 40$ mrad.

$$\frac{\partial f}{\partial x}(x,\Delta E) = \sum_{kn}\int_0^\infty d\sigma_{kn}[f(x,\Delta E-\Delta E_{kn})-f(x,\Delta E)], \tag{1}$$

where ΔE_{kn} is the single collision energy loss due to the excitation of an atomic electron from the discrete state n to the continuum state k, and $d\sigma_{kn}$ the differential cross section for N atoms per unit volume. The Fourier transform of $f(x,\Delta E)$ is written

$$\hat{f}(x,\omega) = \exp[-xg(\omega)],$$

with (2)

$$g(\omega) = \sum_{kn}\int_0^\infty d\sigma_{kn}[1-\exp(-i\omega\Delta E_{kn})].$$

From the Bethe treatment with the Møller correction[20] for the relativistic Born approximation of the scattering of a fast electron,

$$d\sigma_{kn} = \frac{\xi}{x}|\eta_{kn}|^2\frac{E'}{E}dQ\left(\frac{1}{Q^2}-\frac{mc^2(2E-mc^2)}{QE^2(E-mc^2-Q)} + \frac{1}{(E-mc^2-Q)^2}+\frac{1}{E^2}\right), \tag{3}$$

where

$$\xi = \frac{2\pi e^4}{mc^2}\frac{1}{\beta^2}N_A\frac{\rho}{A}x;$$

ρx is the mass thickness, A is the atomic mass, and N_A Avogadro's number. The energies E and E' are the electron energy before and after scattering. In this expression it is a reasonable approximation to set $E'/E \simeq 1$.

$$Q = (1/2m)[\hbar^2q^2-(E-E')^2/c^2],$$

where $\hbar\vec{q} = \vec{p}-\vec{p}'$ is the linear momentum transferred to the atomic electron. η_{kn} is the relativistic form factor. The other notations are conventional.

As suggested by Landau, Eq. (2) is separated into two terms by introducing an intermediate Q value, Q_0, such that for $Q > Q_0$ the energy transferred to an atomic electron is much greater than the atomic-level excitation energy. In this case, it can be shown that

$$Q \simeq \Delta E_{kn} \quad \text{and} \quad |\eta_{kn}|^2 \simeq F_{kn}, \tag{4}$$

where F_{kn} is the oscillator strength associated with the transition $n \to k$. When $Q < Q_0$,

$$|\eta_{kn}|^2 \simeq (F_{kn}/\Delta E_{kn})(Q-\Delta E_{kn}^2/2\gamma^2mc^2), \tag{5}$$

where γ is the relativistic factor.
Hence

$$g(\omega) = g^{(1)}(\omega)+g^{(2)}(\omega). \tag{6}$$

As the lower limit of Q is given by $Q_{\min} = \Delta E_{kn}^2/2\gamma^2\beta^2mc^2$, $g^{(1)}(\omega)$ is written

$$g^{(1)}(\omega) = \frac{\xi}{x}\sum_{kn}\int_{Q_{\min}}^{Q_0}\frac{F_{kn}}{\Delta E_{kn}}\left(Q-\frac{\Delta E_{kn}^2}{2\gamma^2mc^2}\right)\left(\frac{1}{Q^2}+\cdots\right) \times[1-\exp(-i\omega\Delta E_{kn})]\,dQ. \tag{7}$$

In the first approximation, $g^{(1)}(\omega)$ becomes

$$g_1^{(1)}(\omega) = i\omega\frac{\xi}{x}\sum_{kn}\int_{Q_{\min}}^{Q_0}F_{kn}\left(Q-\frac{\Delta E_{kn}^2}{2\gamma^2mc^2}\right)\frac{dQ}{Q^2}, \tag{8}$$

where we have dropped the Møller correction terms because both Q_0 and $Q_{\min}$ are small compared to the incident electron energy.

Introducing the expression of the mean free path for the excitation of the transition $n \to k$, we have

$$g_1^{(1)}(\omega) = i\omega\sum_{kn}\Delta E_{kn}\lambda_{kn}^{-1}. \tag{9}$$

Assuming that the summation on the continuum can be made by taking account of the variation of the generalized oscillator strength like ΔE_{kn}^{-3},[21] it can then be shown that

$$g_1^{(1)}(\omega) = i\omega\sum_n\Delta E_n\lambda_n^{-1}, \tag{10}$$

where λ_n^{-1} is associated with the initial level n and E_n is obtained from the edge ΔE_{0n} by $\Delta E_n = 1.5\Delta E_{0n}$. If F_n is the oscillator strength associated with the n level,

$$\lambda_n^{-1} = \frac{\xi}{x}\frac{F_n}{\Delta E_n}\left[\ln\left(\frac{2\gamma^2\beta^2mc^2Q_0}{\Delta E_n^2}\right)-\beta^2\right]. \tag{11}$$

This formula has been confirmed by our experiments; Q_0 has the value defined by the maximal scattering angle α which is small. Hence,

$$g_1^{(1)}(\omega)=i\omega\frac{\xi}{x}\sum_n\frac{F_n}{\Delta E_n}\left[\ln\left(\frac{2\gamma^2\beta^2mc^2Q_0}{\Delta E_n^2}\right)-\beta^2\right]. \quad (12)$$

This equation can be simplified by considering the sum equation

$$\sum_n F_n=Z, \quad (13)$$

where Z is the number of electrons per atom, and by introducing the mean ionization potential I given by

$$\sum_n F_n\ln\Delta E_n=Z\ln I. \quad (14)$$

Hence

$$g_1^{(1)}(\omega)=i\omega\frac{\xi}{x}Z\left[\ln\left(\frac{2\gamma^2\beta^2mc^2Q_0}{I^2}\right)-\beta^2\right]. \quad (15)$$

The second term in Eq. (6) can be written

$$g^{(2)}(\omega)=\sum_{kn}\int_{Q_0}^{\infty}d\sigma_{kn}[1-\exp(-i\omega\Delta E_{kn})]$$
$$=\frac{\xi}{x}\sum_{kn}\int_{Q_0}^{\infty}F_{kn}d\Delta E_{kn}\left(\frac{1}{\Delta E_{kn}^2}+\cdots\right)$$
$$\times[1-\exp(-i\omega\Delta E_{kn})]. \quad (16)$$

This integral has been calculated by Landau without taking account of the Møller correction terms. The value of $g^{(2)}(\omega)$ is

$$g^{(2)}(\omega)=i\omega\frac{\xi}{x}\sum_{kn}F_{kn}[1-C-\ln(i\omega Q_0)]$$
$$=i\omega(\xi/x)Z[1-C-\ln(i\omega Q_0)], \quad (17)$$

where C is the Euler constant: $C=0.577$.

Finally, by adding (15) and (17), the expression of $g_1(\omega)$, which is the first order of $g(\omega)$, is the same as the one of Landau treatment:

$$g_1(\omega)=g_L(\omega)$$
$$=i\omega(\xi/x)Z[\ln(2\gamma^2\beta^2mc^2/I^2)+1-C-\beta^2]. \quad (18)$$

A. Influence of plasmons

The plasmon creation which is well known in metals can be included in this theory.[22] Unfortunately the expression of the mean free path associated with this excitation is not given by (11). Since plasmon creation is essentially only longitudinal and not partially transversal as in the case of atomic electron excitations, it can be demonstrated that[19]

$$\lambda_p^{-1}=\frac{\xi}{x}\frac{F_1}{E_p}\ln\left(\frac{\hbar q_c v}{1.132E_p}\right)^2, \quad (19)$$

where E_p is the plasmon energy, F_1 the oscillator strength associated with the outer atomic electrons, and q_c the cutoff wave vector. F_1 can be considered as equal to the number Z_V of outer atomic electrons.

Introducing plasmon creation in $g_1^{(1)}(\omega)$, Eq. (8) becomes

$$g_1^{(1)}(\omega)=\frac{i\omega}{x}\left[\xi\sum_{k,n\neq 1}\int_{Q_{\min}}^{Q_0}F_{kn}\left(Q-\frac{\Delta E_{kn}}{2\gamma^2mc^2}\right)\frac{dQ}{Q^2}+\int_{Q_{\min}}^{Q_0}d\sigma_p E_p+\xi\sum_k\int_{Q_c}^{Q_0}F_{k1}\left(Q-\frac{\Delta E_{k1}}{2\gamma^2mc^2}\right)\frac{dQ}{Q^2}\right], \quad (20)$$

where $Q_c=\hbar^2q_c^2/2m$. Then $g_1^{(1)}(\omega)$ can be written

$$g_1^{(1)}(\omega)=\frac{i\omega\xi}{x}\left\{Z\left[\ln\left(\frac{2\gamma^2\beta^2mc^2Q_0}{I^2}\right)-\beta^2\right]+\left|Z_v\ln\left(\frac{\hbar q_c v}{1.132E_p}\right)^2-\sum_k F_{k1}\left[\ln\left(\frac{2\gamma^2\beta^2mc^2\hbar^2q_c^2}{\Delta E_{k1}^2}\right)-\beta^2\right]\right\} \quad (21)$$

or, if we consider that

$$\sum_k F_{k1}\ln\Delta E_{k1}=Z_v\ln\Delta E_1, \quad (22)$$

$$g_1^{(1)}(\omega)=i\omega\frac{\xi}{x}\left[Z\left(\ln\frac{2\gamma^2\beta^2mc^2Q_0}{I^2}-\beta^2\right)+Z_v\ln\left(\frac{\Delta E_1}{1.132\gamma E_p}\right)^2+\beta^2\right]. \quad (23)$$

Hence,

$$g_1(\omega)=g_L(\omega)+g_p(\omega),$$

with

$$g_p(\omega)=i\omega(\xi/x)Z_v[\ln(\Delta E_1/1.132\gamma E_p)^2+\beta^2]. \quad (24)$$

Setting

$$a=\xi Z_v[\ln(\Delta E_1/1.132\gamma E_p)^2+\beta^2],$$

the Fourier transform $\hat{f}_1(x,\omega)$ of the first order energy loss distribution is

$$\hat{f}_1(x,\omega)=\hat{f}_L(x,\omega)\exp(-ia\omega).$$

Thus

$$f_1(x,\Delta E)=f_L(x,\Delta E)*\delta(\Delta E-a)=f_L(x,\Delta E-a), \quad (25)$$

where $\hat{f}_L(x,\omega)$ and $f_L(x,\Delta E)$ are relative to the Landau treatment and * is the convolution operator. In this model, the influence of plasmons is only to shift the Landau distribution. When the electron kinetic energy is 1 MeV and the foil thickness is 3 μm, the factor $a\simeq -20$ eV. This shift towards larger energy losses is smaller

than our experimental uncertainty and is therefore neglected.

B. Influence of quadratic terms

If the exponential term in $g_1^{(1)}(\omega)$ is expanded to the second-order term, as proposed by Blunck and Leisegang, $g(\omega)=g_2(\omega)$ with

$$g_2(\omega)=g_1(\omega)+\tfrac{1}{2}\omega^2\frac{\xi}{x}\sum_{kn}\int_{Q_{\min}}^{Q_0}\Delta E_{kn}F_{kn}\times\frac{1}{Q^2}\left(Q-\frac{\Delta E_{kn}^2}{2\gamma^2mc^2}\right)dQ,$$

and by summing over the k states,

$$g_2(\omega)=g_1(\omega)+\tfrac{1}{2}\omega^2\sum_{kn}\Delta E_{kn}^2\lambda_{kn}^{-1}=g_1(\omega)+\tfrac{1}{2}\omega^2\sum_{n}\Delta E_n^2\lambda_n^{-1}. \quad (26)$$

Following those authors

$$\overline{K_r^2}\equiv\sum_n\Delta E_n^2\lambda_n^{-1}$$

and

$$g_2(\omega)=g_1(\omega)+\tfrac{1}{2}\omega^2\overline{K_r^2}. \quad (27)$$

Thus,

$$\hat{f}_2(x,\omega)=\hat{f}_1(x,\omega)\exp(-\tfrac{1}{2}x\omega^2\overline{K_r^2})$$

and

$$f_2(x,\Delta E)=f_1(x,\Delta E)*[1/(2\pi x\overline{K_r^2})^{1/2}]\times\exp(-\Delta E^2/2x\overline{K_r^2}). \quad (28)$$

The second-order distribution $f_2(x,\Delta E)$ is a convolution of the first-order distribution $f_1(x,\Delta E)$ by a Gauss function defined by $\overline{K_r^2}$. The main result is an enlargement of $\Delta E_{1/2}$. Figure 4 shows this effect in the case of aluminum. The influence of plasmons in $\overline{K_r^2}$ is negligible due to the low value of the associated energy loss. The Landau distribution used is the one recently tabulated by Borsch-Supan.[23] On the other hand, ΔE_p is increased because the Gauss function is a symmetric one alike the Landau distribution.

Since our experiments show a systematically lower value of the enlargement of the straggling distribution and of the most probable energy loss as compared to the Blunck and Leisegang theory, we have attempted to explain them by considering the contribution of all higher-order terms.

C. Influence of higher-order terms

If we expand the exponential term in $g^{(1)}(\omega)$ up to the M order, we obtain

$$g_M(x,\omega)=g_L(\omega)-\sum_{m=2}^{M}\frac{(-i\omega)^m}{m!}\sum_{kn}\int_{Q_{\min}}^{Q}\frac{\xi}{x}\times\Delta E_{kn}^{m-1}F_{kn}\left(Q-\frac{\Delta E_{kn}^2}{2\gamma^2mc^2}\right)\frac{dQ}{Q^2}$$

$$=g_L(\omega)-\sum_{m=2}^{M}\frac{(-i\omega)^m}{m!}\sum_{kn}\Delta E_{kn}^m\lambda_{kn}^{-1}$$

$$=g_L(\omega)-\sum_{m=2}^{M}\frac{(-i\omega)^m}{m!}\sum_{n}\Delta E_n^m\lambda_n^{-1}. \quad (29)$$

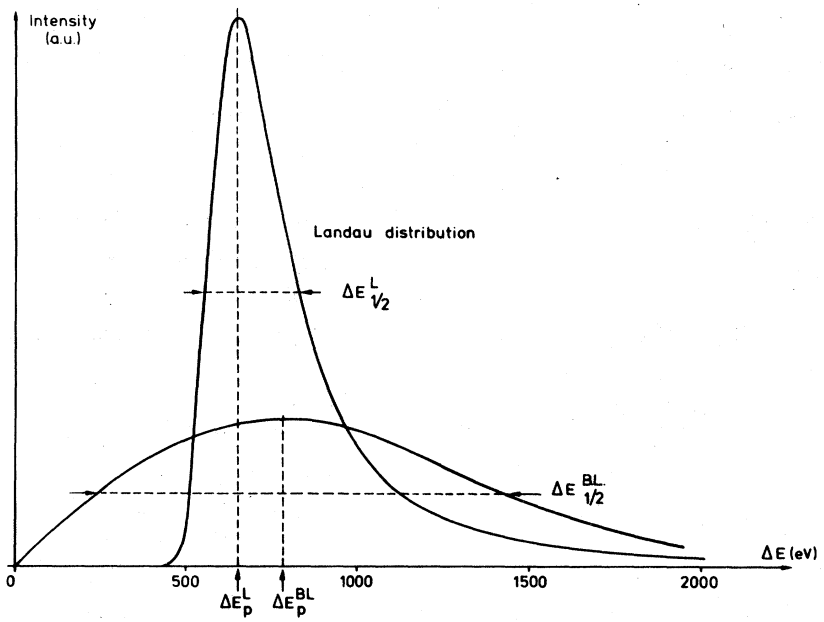

FIG. 4. Influence of the Blunck and Leisegang correction on the Landau distribution in the case of a 3-μm-thick aluminum foil at 1 MV.

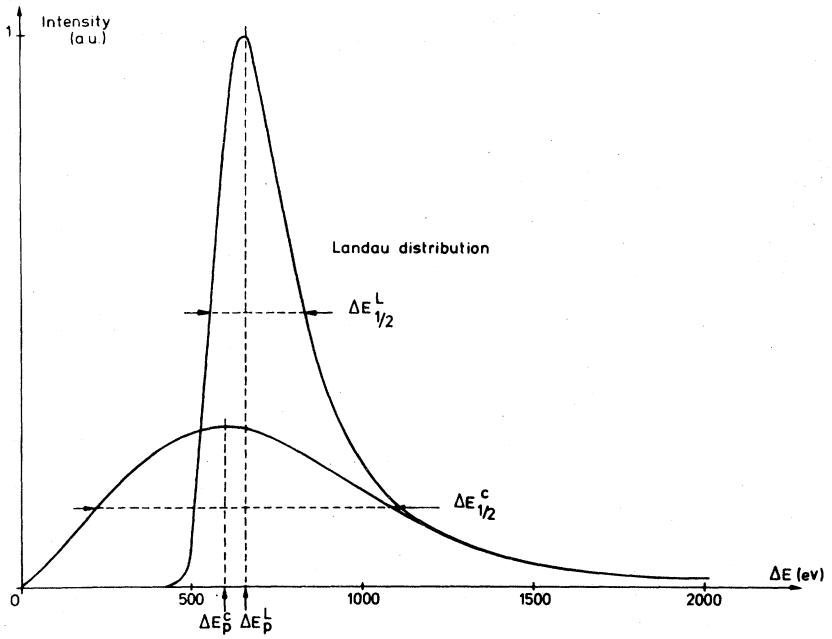

FIG. 5. Influence of the all order term correction on the Landau distribution in the same case as in Fig. 3.

Hence,

$$g(x,\omega) = g_L(\omega) + \sum_n \lambda_n^{-1}[1 - \exp(-i\omega\Delta E_n)] - i\omega \sum_n \Delta E_n \lambda_n^{-1} . \quad (30)$$

Writing

$$g_c(\omega) \equiv \sum_n \lambda_n^{-1}[1 - \exp(-i\omega\Delta E_n)] - i\omega \sum_n \Delta E_n \lambda_n^{-1} \quad (31)$$

and

$$\hat{f}_c(\omega) = \exp[-x g_c(\omega)] ,$$

we obtain

$$f(x,\Delta E) = f_L(x,\Delta E) * f_c(x,\Delta E) . \quad (32)$$

This equation shows that the complete distribution $f(x,\Delta E)$ is deduced from the Landau one by convoluting with a correction function $f_c(x,\Delta E)$ which takes into account all order terms. This function is a generalization ot the Blunck and Leisegang correction and can be computed numerically. Figure 5 shows the influence of the correction in the case studied in Fig. 4. As compared to the Landau distribution, ΔE_p is shifted towards lower-energy losses and the increase of $\Delta E_{1/2}$ is smaller than the one given by the Blunck and Leisegang correction.

IV. COMPARISON WITH EXPERIMENTS

As the thickness of the samples increases, the characteristic distributions due to plasmons and inner-shell excitations vanish progressively into the background and the energy-loss spectra can be compared to the Landau distribution. The microdensitometer traces of Figs. 6(a)–6(c) show this modification for 0.76–8.5-μm-thick aluminum foils and 1-MeV incident electrons; Fig. 6(d) shows the variation of straggling for 0.3-, 0.75-, 1.2-MeV incident electrons transmitted through the same 3-μm-thick aluminum foil. As can be seen in Fig. 6(d), the chromatic aberration on the electron micrographs decreases with increasing accelerating voltage. We have determined ΔE_p and $\Delta E_{1/2}$ from these spectra. In Tables I and II, experimental values of $\Delta E_p^{\exp}$ are compared to the values deduced from the Landau treatment ΔE_p^L and from the corrected treatment ΔE_p^c. These results are shown in Figs. 7(a) and 7(b) and in Table I.

The experimental determination of ΔE_p is easy and the accuracy is mainly limited by the precision of thickness measurements. We observe that experimental values are systematically 10 or 20% lower than Landau's ones. With the correction which takes account of all orders, we get calculated values of ΔE_p within the probable error of the experiments.

Concerning $\Delta E_{1/2}$, the measurements are more critical. They can be affected by the nonlinearity of the photographic technique. The precision can be evaluated at ±10%. There is a large discrepancy between the observed values and the calculated Landau's ones. These latter are two or three times lower than the experimental values. The

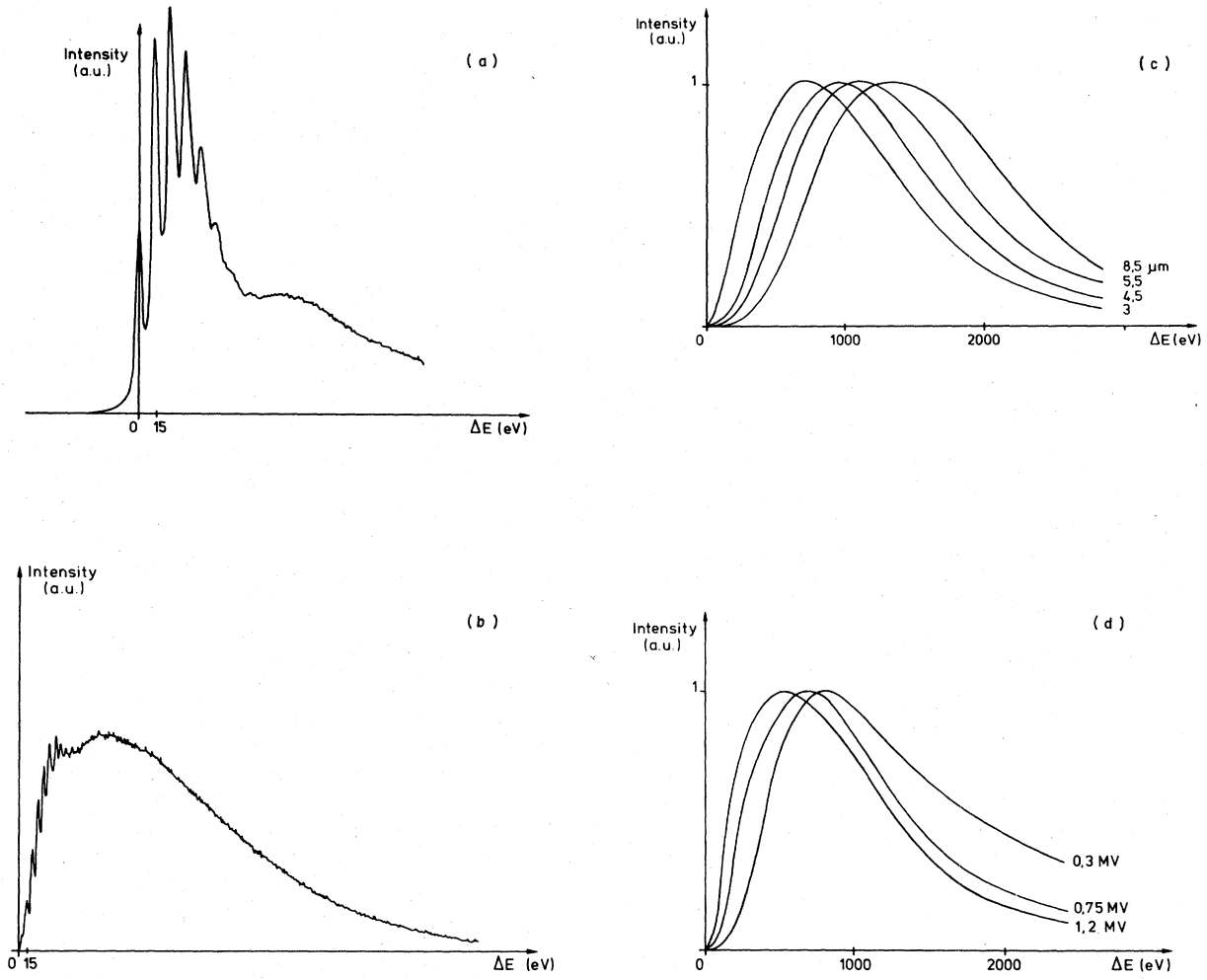

FIG. 6. Electron-energy-loss spectra through aluminum foils for various thicknesses x. (a) $x = 0.76\ \mu$m, $V = 1$ MV; (b) $x = 2\ \mu$m, $V = 1$ MV; (c) $x = 3$, 4.5, 5.5, 8.5 μm, $V = 1$ MV; (d) $x = 3\ \mu$m, $V = 0.3$, 0.75, 1.2 MV.

Blunck-Leisegang correction reduces the discrepancy but gives values about 30% too large. Figures 8(a) and 8(b) and Table II show that, by introducing all the correction orders, the experimental values are in better agreement.

The influence of plasmon multiple scattering is also very weak: the most probable energy loss calculated by multiple plasmon scattering as suggested by Hirsch and Humphreys[24] would be much smaller than ΔE_p: for instance, with 3-μm alu-

TABLE I. Most probable energy loss in aluminum for different foil thicknesses and different accelerating of incoming electrons. ΔE_p^L, ΔE_p^c, and ΔE_p^{exp} are the Landau, corrected and experimental values, respectively.

	$x = 3\ \mu$m			$x = 5.5\ \mu$m			$x = 8.5\ \mu$m		
V_{kV}	ΔE_p^L (eV)	ΔE_p^c (eV)	ΔE_p^{exp} (eV)	ΔE_p^L (eV)	ΔE_p^c (eV)	ΔE_p^{exp} (eV)	ΔE_p^L (eV)	ΔE_p^c (eV)	ΔE_p^{exp} (eV)
300	824	784	770	1621	1585	1360	2628	2572	2400
500	691	611	640	1357	1298	1250	2197	2105	1950
750	641	584	540	1255	1202	1210	2058	1947	1840
1000	626	545	520	1242	1149	1190	1974	1784	1720
1200	618	532	540	1216	1120	1040	1961	1820	1660

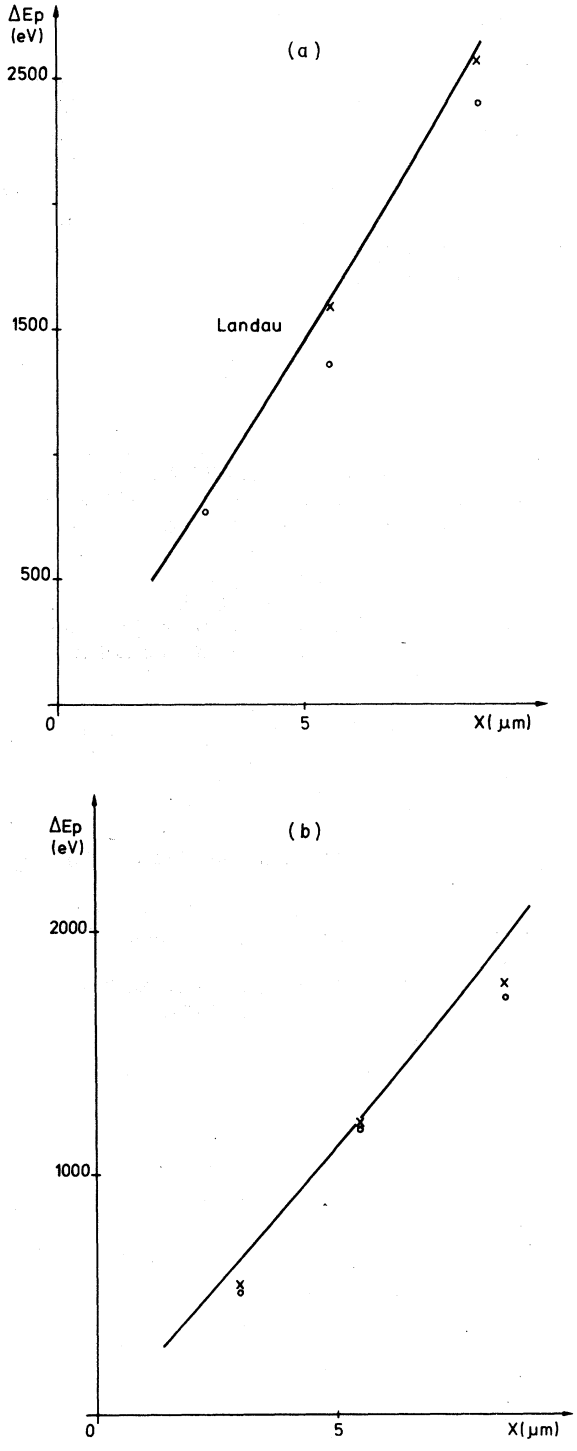

FIG. 7. Variation of the most probable energy loss ΔE_p of electrons as a function of aluminum foil thickness x. The solid curve corresponds to the Landau theory; ○ are the experimental values and × are our own corrected values. (a) $V = 0.3$ MV; (b) $V = 1$ MV.

TABLE II. Full width at half maximum of the energy-loss distribution in aluminum for different foil thicknesses and different accelerating of incoming electrons. $\Delta E^L_{1/2}$, $\Delta E^c_{1/2}$, and $\Delta E^{exp}_{1/2}$ are the Landau, corrected, and experimental values, respectively.

	$x = 3$ μm			$x = 8.5$ μm		
V_{kV}	$\Delta E^L_{1/2}$ (eV)	$\Delta E^c_{1/2}$ (eV)	$\Delta E^{exp}_{1/2}$ (eV)	$\Delta E^L_{1/2}$ (eV)	$\Delta E^c_{1/2}$ (eV)	$\Delta E^{exp}_{1/2}$ (eV)
300	401	1092	940	1136	1974	
500	325	1002	920	920	1820	1950
750	289	967	890	820	1743	1816
1000	273	922	870	774	1715	1730
1200	265	969	820	752	1720	

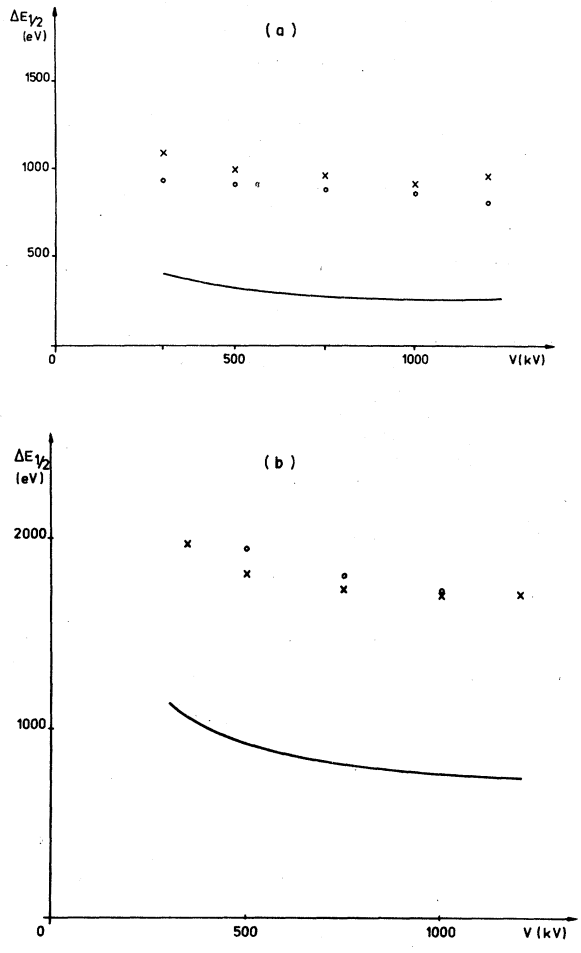

FIG. 8. Variation of the width at half height of the electron-energy-loss distribution $\Delta E_{1/2}$ as a function of the accelerating voltage V in aluminum. The solid curve corresponds to the Landau theory; ○ are the experimental values and × are our own corrected values. (a) $x = 3$ μm; (b) $x = 8.5$ μm.

minum foils, at 1 MeV, ΔE_p due to plasmons is about 150 eV.[19]

Analogous experimental results, which are in good agreement with the calculated ones by a Monte Carlo method,[25] have recently been obtained in the case of a gas sample.[10]

V. SUMMARY

Finally the experimental values of the most probable energy loss and the width at half maximum allow one to conclude that the free-electron model proposed by Landau with the correction including all order resonant terms is a good approximation of the scattering processes of electrons through aluminum. The density effect, Bremsstrahlung, and Cerenkov radiation are negligible for this light element and this incident energy range. These results confirm that individual collisions by ionization and excitation are the main scattering processes of electrons through matter.

[1]D. W. Aitken, W. L. Lakin, and H. R. Zulliger, Phys. Rev. 179, 393 (1969).
[2]H. Bichsel, Nucl. Instrum. Methods 78, 277 (1970).
[3]J. J. Kolata, T. M. Amos, and H. Bichsel, Phys. Rev. 176, 484 (1968).
[4]H. O. Maccabee, M. R. Raju, and C. A. Tobias, Phys. Rev. 165, 469 (1968).
[5]E. H. Bellamy, R. Hofstadter, W. L. Lakin, J. Cox, M. L. Perl, W. T. Toner, and T. F. Zipf, Phys. Rev. 164, 417 (1967).
[6]J. J. L. Chen and S. O. Warshaw, Phys. Rev. 84, 355 (1951).
[7]E. L. Goldwasser, F. E. Mills, and A. O. Hanson, Phys. Rev. 88, 1137 (1952).
[8]L. Landau, J. Phys. USSR 8, 201 (1944).
[9]P. V. Vavilov, Sov. Phys.-JETP 5, 749 (1957).
[10]K. Nagata, A. Kuge, A. Nakamoto, N. Hasebe, J. Kikuchi, and T. Doke, J. Phys. D 9, 1907 (1976).
[11]O. Blunck and S. Leisegang, Z. Phys. 128, 500 (1950).
[12]K. Considine, K. C. A. Smith, and V. E. Cosslett, Proceedings of the Seventh International Congress on Electron Microscopy Grenoble (1970), Vol. 2, p. 131 (unpublished).
[13]J. Sevely, J. Ph. Perez, and B. Jouffrey, C. R. Hebd. Séanc. Acad. Sci. Paris, 276, 515 (1973).
[14]G. Dupouy and F. Perrier, J. Microsc. 1, 167 (1962).
[15]S. M. Seltzer and M. J. Berger, Natl. Acad. Sci.-Nat. Resl. Counc. Publ. 433, 187 (1964).
[16]H. Bichsel, Phys. Rev. B 7, 2854 (1970).
[17]H. Bichsel, Phys. Rev. A 9, 571 (1974).
[18]J. Sevely, J. Ph. Perez, and B. Jouffrey, Third International Conference on H. V. E. M., Oxford 32 (1973) (unpublished).
[19]J. Ph. Perez, Thèse (Toulouse, 1976) (unpublished).
[20]H. Bethe, *Handbuch der Physik* (Springer, Berlin, 1933), XXIV/I, p. 491.
[21]H. A. Bethe and R. W. Jackiw, *Intermediate Quantum Mechanics* (Benjamin, New York, 1968).
[22]C. J. Humphreys (private communication).
[23]W. Borsch-Supan, J. Res. Natl. Bur. Stand. (U.S.) B 65, 245 (1961).
[24]P. B. Hirsch and C. J. Humphreys, Fourth European Reg. Conference Electron Microscopy, Rome (1968), Vol. 1, p. 49 (unpublished).
[25]K. A. Ispirian, A. T. Margaryan, and A. M. Zverev, Nucl. Instrum. Methods 117, 125 (1974).

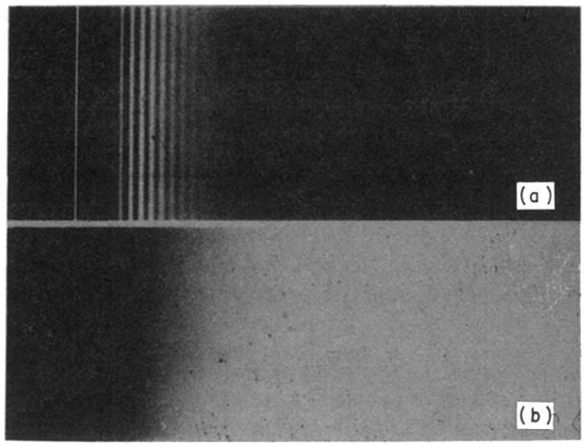

FIG. 3. Influence of the maximal scattering angle on the energy-loss spectra obtained with samples a few microns thick: Electron kinetic energy, 1 MeV; thickness, 3 μm. (a) $\alpha = 0.5$ mrad. In this micrograph the no loss line has been superimposed in the spectrum; (b) $\alpha = 40$ mrad.